

# The modulation ratio in comprehensive two-dimensional gas chromatography: a review of fundamental and practical considerations

## *A razão de modulação em cromatografia gasosa bidimensional abrangente: uma revisão de aspectos fundamentais e práticos*

Philip John Marriott<sup>1\*</sup>

Carin von Mühlen<sup>2</sup>

<sup>1</sup>Australian Centre for Research on Separation Science, School of Chemistry, Monash University, Clayton, Victoria 3800, Australia

<sup>2</sup>Departamento de Química e Ambiental, Faculdade de Tecnologia, Universidade do Estado do Rio de Janeiro, Rodovia Presidente Dutra, Km 298, Resende, Cep 27537-000, Rio de Janeiro, Brasil

\*philip.marriott@monash.edu

**Recebido:** 25-02-2016

**Aceito:** 27-04-2016

### Abstract

This paper presents a discussion on the implications of the modulation ratio ( $M_R$ ) in comprehensive two-dimensional gas chromatography (GC×GC) separations. Concepts are discussed in a tutorial manner, which is essentially in the form of a review. The  $M_R$  is defined as the ratio of the width of a peak as it elutes from a first dimension (<sup>1</sup>D) column, to the modulation period used in GC×GC operation; it is a dimensionless number. As demonstrated here, there are many parameters of GC×GC that depend on or can be interpreted by considerations of the  $M_R$  value. These include, but are not limited to, the peak amplitude enhancement, the number of modulated peaks that are observed, detectivity of each of these peaks, the effect of chromatographic peak shape on the distribution of modulated peaks and how peak retention time on the first column can be derived from this distribution. Also considerations of the physical dimensions and phase coating of the second (<sup>2</sup>D) column that is used in GC×GC (these control the total retention time of the peaks on the <sup>2</sup>D column) can be interpreted based on the  $M_R$ , and how knowledge of this parameter can assist in interpretation of the separation of isomers.

**Keywords:** Modulation ratio; comprehensive two-dimensional gas chromatography; quadrupole mass spectrometry; quantification.

### Resumo

Esse artigo apresta uma discussão sobre as implicações da razão de modulação ( $M_R$ ) na cromatografia gasosa bidimensional abrangente (GC×GC). Os conceitos foram discutidos em formato tutorial, que é essencialmente uma revisão da literatura. A  $M_R$  é definida como a razão entre a largura do pico eluído da coluna da primeira dimensão (<sup>1</sup>D) e o período de modulação usado na operação do GC×GC em número adimensional. Como demonstrado aqui, existem muito parâmetros de GC×GC que são dependentes ou podem ser interpretados por considerações relativas ao valor da  $M_R$ . Dentre eles, destacam-se o aumento da amplitude do pico, o número de modulações por pico observada, a detectabilidade de cada um desses picos, o efeito do formato do pico sobre a distribuição dos picos modulados e como o tempo de retenção dos picos monodimensionais pode ser derivada dessa distribuição. Também serão discutidas considerações sobre como as dimensões físicas e a fase de recobrimento da segunda coluna (<sup>2</sup>D) usada em GC×GC (isso controla o tempo de retenção total dos picos na coluna <sup>2</sup>D) podem ser interpretadas com base na  $M_R$ , e como esse parâmetro pode auxiliar na interpretação da separação de isômeros.

**Palavras-chave:** razão de modulação; cromatografia gasosa bidimensional abrangente, espectrometria de massas quadrupolar, quantificação.

## 1. Introduction

Since its inception in 1991<sup>[1]</sup>, comprehensive two-dimensional gas chromatography (GC×GC) has adopted a key position in the technology of multidimensional gas chromatography (MDGC) because of its high resolution, and its innovative ability to provide a complete 2D picture – 3D if detection response is added – of samples<sup>[2,3]</sup>. Many unique aspects of GC analysis derive from the application of GC×GC, and a new terminology has been developed to cater for this method<sup>[4,5]</sup>. Amongst these, is the concept of modulation ratio ( $M_R$ ).

The modulation ratio in GC×GC<sup>[6-9]</sup> is defined as (Eq. 1):

$$M_R = \frac{4 \cdot \sigma}{P_M} = \frac{\left( \frac{4 \cdot w_b}{2.54} \right)}{P_M} \quad (1)$$

This expression relates the width of the first dimension (<sup>1</sup>D) peak in terms of its standard deviation ( $\sigma$ ) to the modulation period ( $P_M$ ) employed in the experiment. Since this expression uses  $4\sigma$ , which is essentially the peak width extrapolated to baseline ( $w_b$ ), then it can be equated to how many modulations are performed per peak width at base. The expression uses  $w_b$  as the experimentally measured variable, since it is easier to measure than the formal width at base, which requires extrapolation through the peak inflexion points. Conversion from  $w_b$  to  $w_h$  requires the factor 2.54. Rather simplistically, it can be interpreted that a  $M_R$  value of 4 generates 1 modulation event per peak standard deviation, i.e. about 4 modulated peaks per peak width at base.

This has a practical outcome that a  $M_R$  value of 4 should produce about 4 ‘reasonably sized’ modulated peaks, but as has been discussed<sup>[7]</sup> this very much depends on factors such as the abundance of the compound, and the modulation phase which describes the particular sampling pattern of the <sup>1</sup>D peak<sup>[6]</sup>. The  $M_R$  value can assist in determination of the length and other physical dimensions and conditions, and maximum elution time desired for the <sup>2</sup>D column<sup>[7]</sup>. One of the primary concerns of GC×GC practitioners is the number of peaks one might

obtain for a given solute. It is desirable to neither over sample nor under sample the primary peaks. Too many modulations (too short a  $P_M$ ) reduces the space between modulations and limits the number of peaks that can be located between successive modulations; oversampling reduces detectability of the compound by reducing the amount of sample in the modulated fraction, and may increase wrap around. Too few modulations risks reducing the apparent resolution on the <sup>1</sup>D column and may reduce resolution on the <sup>2</sup>D column if two peaks are captured into a common sampling event and cannot be resolved on the <sup>2</sup>D column. Overloading of the second dimension column is also more likely to occur<sup>[10]</sup>.

In-phase modulation produces a single major peak, with a symmetric distribution of lower intensity minor pulses as the extremities away from the peak maximum are sampled. 180° out-of-phase modulation produces two major peaks distributed symmetrically about the peak maximum, at exactly 0.5 of the  $P_M$  value, and again with minor modulated peaks that decrease monotonically along the extremities of the sampled <sup>1</sup>D peak. Between these two extreme cases, the modulated peak pattern describes an asymmetric shape. This will be further considered below.

As an input peak decreases in response magnitude, then clearly the modulated peaks in the GC×GC experiment will correspondingly decrease in response height. In order to be effectively quantified, each pulse should be greater than a given response, corresponding to the limit of quantification. This has the effect of reducing the number of modulated peaks that are summed in order to represent the total area of the input peak. Hence, for abundant components, more minor peaks may be summed in order to deduce the original peak area, but for low abundance <sup>1</sup>D peaks, the modulated pulses at the extremities of the distribution are increasingly likely to be less than the quantification limit. This immediately poses some interesting scenarios. Clearly in some cases (of low abundance components), a greater proportion of the component area will be neglected, since it will be less than the quantification limit. The idea of using a

given number of modulated peaks to represent a reliable proportion of the component was examined by Amador-Muñoz and Marriott<sup>[9]</sup>, who reported a study where either the 2 or 3 maximum modulated peaks were tested to be summed, in a study of PAH sampled from urban air, with deuterated PAH providing comparative quantification. This metric clearly could be sensitive to the modulation phase, especially where  $P_M$  is low, and the analyte is in low amounts.

Another question arises. For qualitative analysis, the maximum peak pulse should be most accurately measured in a mass spectrometer – it should give the best library match (but may not necessarily give the highest match quality!) If each of the modulated pulses is of the same well-resolved compound, then they should also give acceptable library matches until the presence of background ions make library matching poor, and low ion abundances unreliable. The question arises as to how many of the minor pulses might be reliably recorded with similar ion abundances over the given mass range.

The modulated peak distribution itself should closely describe a Gaussian peak, reflecting the shape of the input  $^1D$  peak at the end of the  $^1D$  column<sup>[11]</sup>. For instance, assuming that the  $P_M$  value exactly corresponds to  $^1\sigma$ , then the cumulative summation of the Gaussian distribution should then correspond to individual peaks whose maxima define a Gaussian shape. Thus a Gaussian distribution may be fitted to the modulated peak maxima. If this is the case, then it is possible to predict reasonably well the retention time of a component on the  $^1D$  column, by modelling the Gaussian shape to identify the peak maximum, taking into account the  $P_M$  value that in cryogenic systems corresponds to the time during which the analyte is held in the trapping region, assessing the presence of any wrap-around, and calculating the  $^2D$  retention time ( $^2t_R$ ). This has been reported elsewhere<sup>[12,13]</sup>, and gives a retention reliability of better than 1 s for the predicted  $^1t_R$ . An interesting point may be made with respect to the anticipated efficiency of modulation and the effect of sampling on resolution and peak capacity. The total peak capacity of a GC×GC experiment is taken

to be the product of the capacities of the two independent dimensions,  $^1D$  and  $^2D$ . But the loss of resolution as a result of the modulation process leads to a reduction in this total, giving about 60% of the  $^1n_c \times ^2n_c$  value. However, since an accurate  $^1t_R$  value can be predicted, this should return to the GC×GC experiment a much greater overall efficiency than that above.

In the present work, we evaluate a number of both previously reported and unreported observations, which further define the general relationships between  $M_R$ , number of summed modulated peaks, and detectability of compounds with consistency of ion ratios, Gaussian peak distributions and sampling rate which determines  $M_R$ .

## 2. Experimental

The research presented here arises from research drawn from various sources, all which relate to ideas of modulation ratio and detection in GC×GC. Not all experimental conditions are presented nor are required for demonstration of the principles of the GC×GC process, but some settings are reproduced in this Section. The most important features are the chromatographic data presented based on the effects of modulation, and interpreted according to the resulting  $M_R$  values.

All chromatographic data were obtained using a longitudinally modulated cryogenic system (LMCS)<sup>[14]</sup>. This system was the first to employ a cryogenic (sub-ambient) cooling fluid – in this case liquid CO<sub>2</sub> which expands to provide the cooling effect – to demonstrate applicability to GC×GC<sup>[15]</sup>. It has also been employed for a range of multidimensional gas chromatography (MDGC) methods<sup>[16]</sup>. The concepts presented here are expected to be valid for other types of modulators, if the different modulators are able to faithfully follow the input (Gaussian) profile of the 1D peak, and have a precisely controlled modulation period.

The Figure 1 data were obtained using FID detection on a dual-column arrangement comprised of a primary column of 25 m × 0.22 mm i.d. with a 1.0 μm film thickness (BPX5-coated column, 5% phenyl-dimethyl

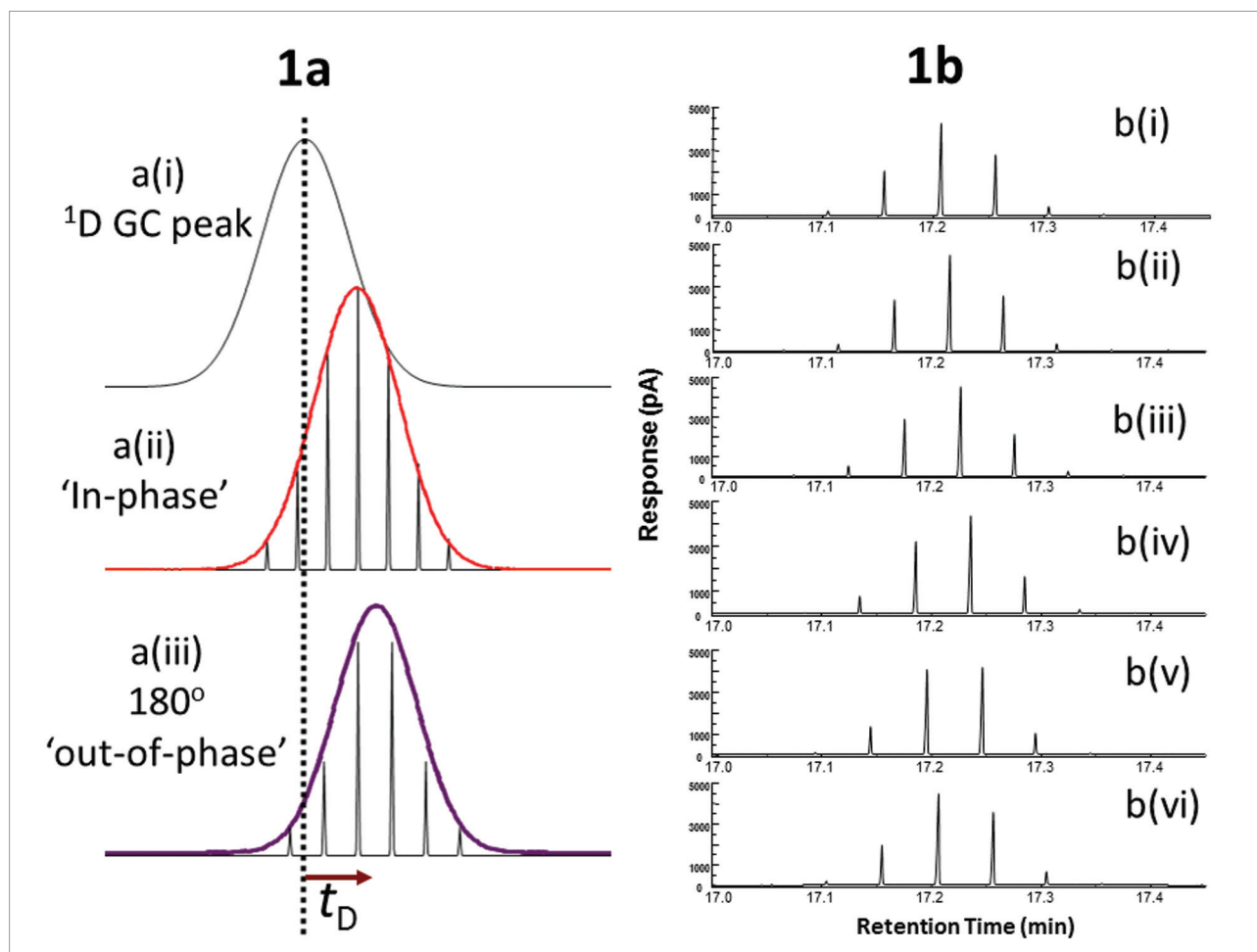


**Figure 1.** Illustration of modulated peak patterns. a(i) a  $^1\text{D}$  peak, with a(ii) in-phase and a(iii) out-of-phase modulation. Peak delay time  $t_D$  corresponds to cryogenic hold-up, equal to  $P_M$  and  $^2t_R$  retention. (b) Peak patterns for different commencement times of modulation, altered by 0.01 min (0.6 s) for a  $3 s P_M$  setting, to permit different patterns to be displayed. b(ii) corresponds closely to in-phase modulation; (b(v)) corresponds closely to  $180^\circ$  out-of-phase modulation; hence (b(ii)) and (b(v)) should differ by close to  $P_M/2$ ; (b(i)) and (b(vi)) differ by 3 s and so should be the same phase.

siloxane phase, nonpolar) directly connected to a short second column of 1.2 m  $\times$  0.1 mm i.d. with a 0.1  $\mu\text{m}$  film thickness (BPX50-coated column, 50% phenyl equivalent polysilphenylene phase, polar) was used for all studies. Both columns used were manufactured by SGE International (Ringwood, Australia). Linalyl acetate was used as analyte to demonstrate the effect of different phase of modulation. The GC oven was operated under a temperature program rate of 60  $^\circ\text{C}$  (held for 1 min) heated to 120  $^\circ\text{C}$  at 20  $^\circ\text{C}/\text{min}$ , then to 150  $^\circ\text{C}$  at 2  $^\circ\text{C}/\text{min}$ , and finally to 180  $^\circ\text{C}$  at 20  $^\circ\text{C}/\text{min}$ . This temperature program was used to give a suitable peak width such that a range of modulation frequencies could be used to study the effect of this variable (i.e., giving a

number of pulsed peaks for the intermediate frequency chosen) and permit a number of modulation start times incremented by 0.01 min to be used.

Figure 2 data came from a multi-component sample conducted under isothermal analysis. The analyte was an alkane, chosen so as to generate a nicely symmetric (Gaussian) peak. Modulation was conducted under different  $P_M$  settings, as shown in the Figure caption.  $M_R$  values are also presented, the calculation of which is aided by the relative width of the peak on the  $^1\text{D}$  column. FID detection was used.

Figure 3 shows a volatile sample of at least 13 components, which in 1D GC analysis appears to display 11 clear peaks. However two peaks recorded

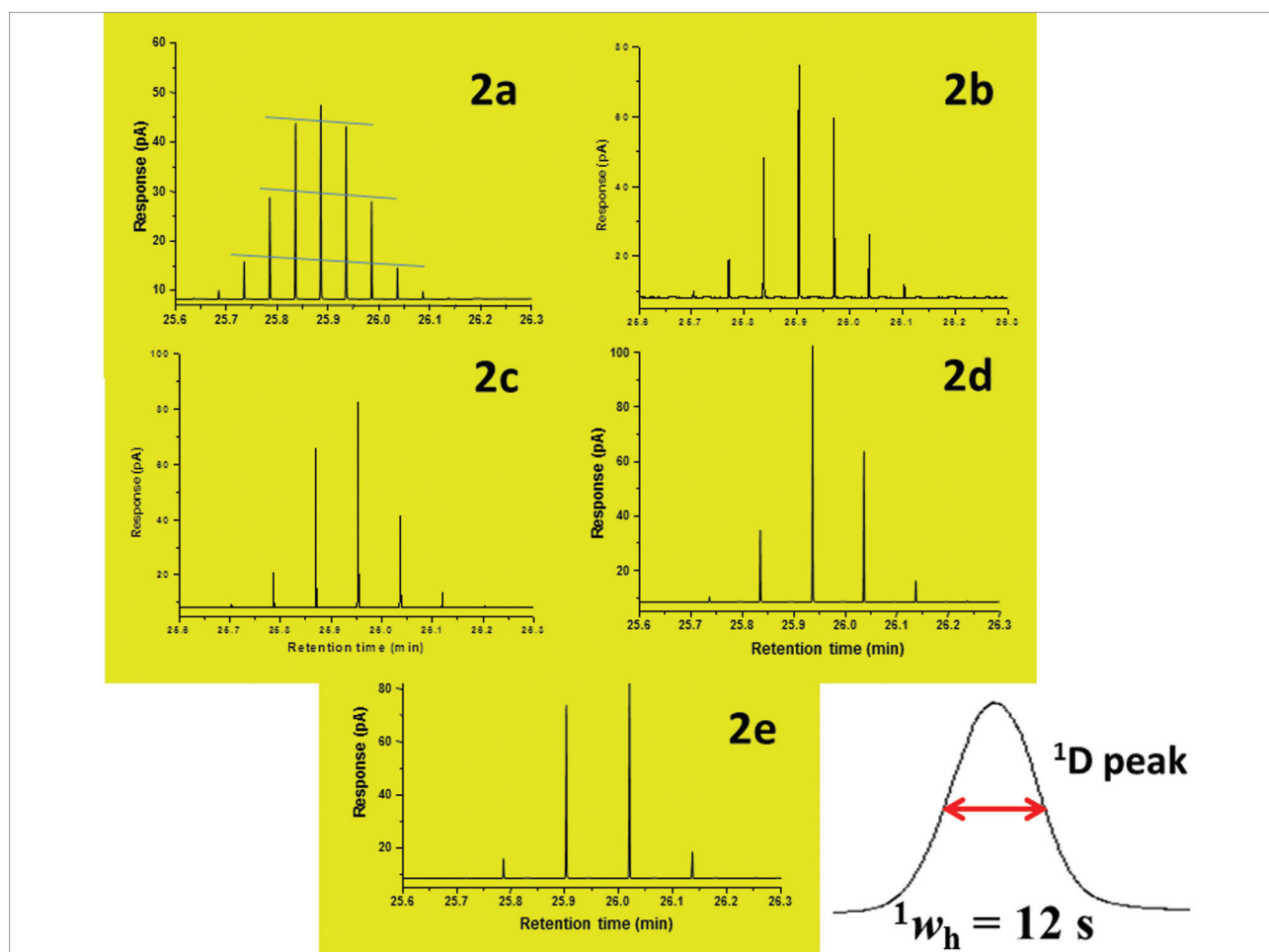
by FID detection are mixtures of two components. The effects of both improved resolution – the overlapping peaks from 1D analysis are now clearly resolved in the modulated result – and also improved peak response – a diluted sample gives considerably improved peak height response for the modulated peaks.

Figure 4 data were obtained for derivatised histidine amino acid, conducted under temperature programming analysis on a column set of <sup>1</sup>D non-polar stationary phase, and <sup>2</sup>D 50% phenyl methyl stationary phase. FID detection was employed. The histidine peak is seen to overlap with an unknown interfering peak.

Figure 5 displays a sample mix containing p-nitroaniline and diphenylamine. The experiment was conducted using quadrupole mass spectrometry, with

a scan acquisition rate of about 20 scans/s. An Agilent model 6890 GC with a LMCS modulator was used, with a mass scan range of 45-250 *m/z*. Figure 5c illustrates that peaks elute within about 7 scans.

Figure 6 is a sample of terpinene-4-ol, with about 70% (+) antipode, and 30% (-) antipode. The first chiral column was an Astec CHIRALDEX B-PM (30 m × 0.25 mm × 0.12 μm df; Supelco) column as <sup>1</sup>D and a SUPELCOWAX10 column (1.0 m × 0.1 mm × 0.1 μm df; Supelco) as <sup>2</sup>D. Oven temperature program was 50 °C (hold 0.2 min) to 80 °C at 10 °C min<sup>-1</sup>, then to 93 °C at 3 °C min<sup>-1</sup>, followed by 5 °C min<sup>-1</sup> to 115 °C, then to 124 °C at 2 °C min<sup>-1</sup> and 20 °C min<sup>-1</sup> to 180 °C. Different  $P_M$  settings were employed, resulting in the data in Figure 6b, translated into a 2D plot in Figure 6c.



**Figure 2.** Altered modulation periods ( $P_M$ ) leading to different modulation ratios ( $M_R$ ) for an isothermal elution <sup>1</sup>D peak of  ${}^1w_h = 12$  s and  ${}^1t_R \sim 25.8$  min. (a)  $P_M = 3$  s,  $M_R = 6.8$ ; (b)  $P_M = 4$  s,  $M_R = 5.1$ ; (c)  $P_M = 5$  s,  $M_R = 4.1$ ; (d)  $P_M = 6$  s,  $M_R = 3.4$ ; (e)  $P_M = 7$  s,  $M_R = 2.7$ . These appear to give ‘numbers of modulated peaks’  $n_M$  of 9, 7, 7, 5 and 4 respectively.

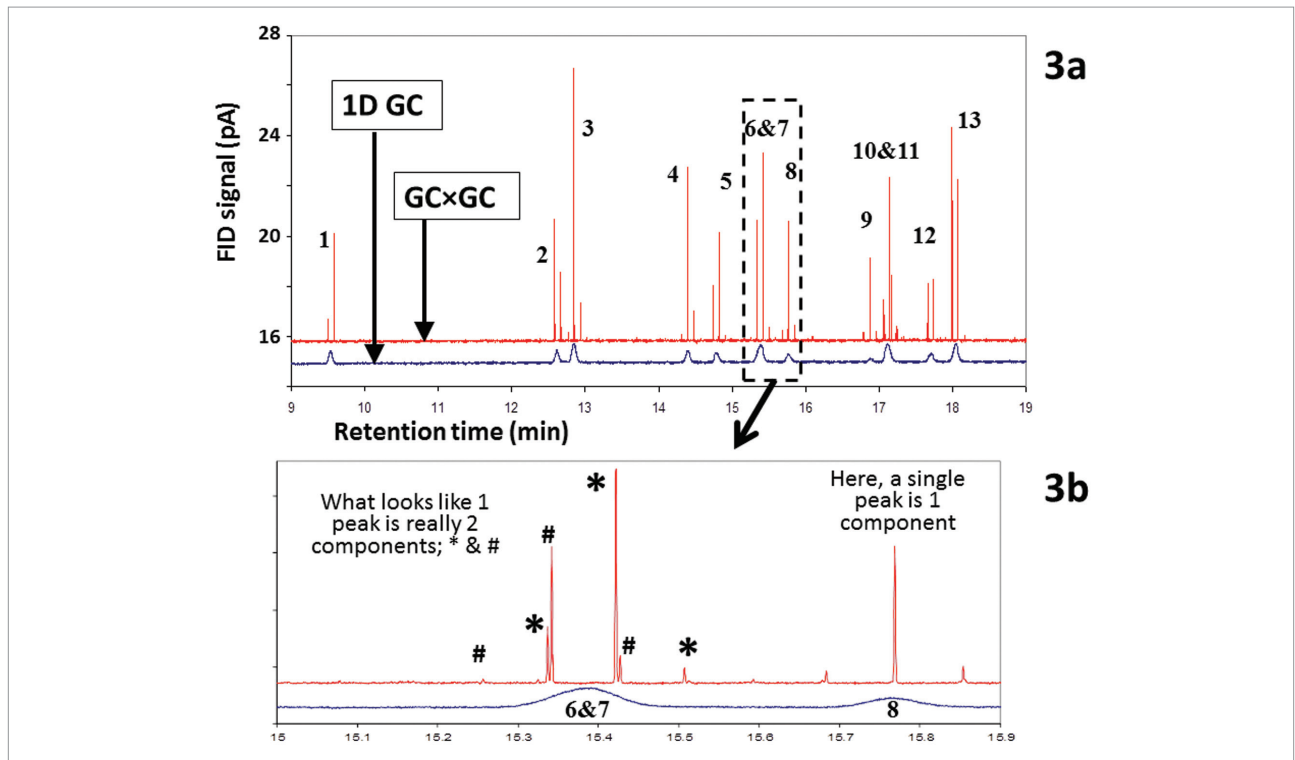


**Figure 3.** (a) The 1D GC result here has a very low response, close to the detection limit as indicated by the noise level. The GC×GC result is obtained with a 2.5-fold reduced concentration, but still is many times increased in response height, by approximately 12-fold. This corresponds to about 30-fold increase in signal magnitude. (b) Peaks 6 & 7 overlap in the 1D GC analysis, but are clearly resolved in the GC×GC result, giving components indicated by # and \*.

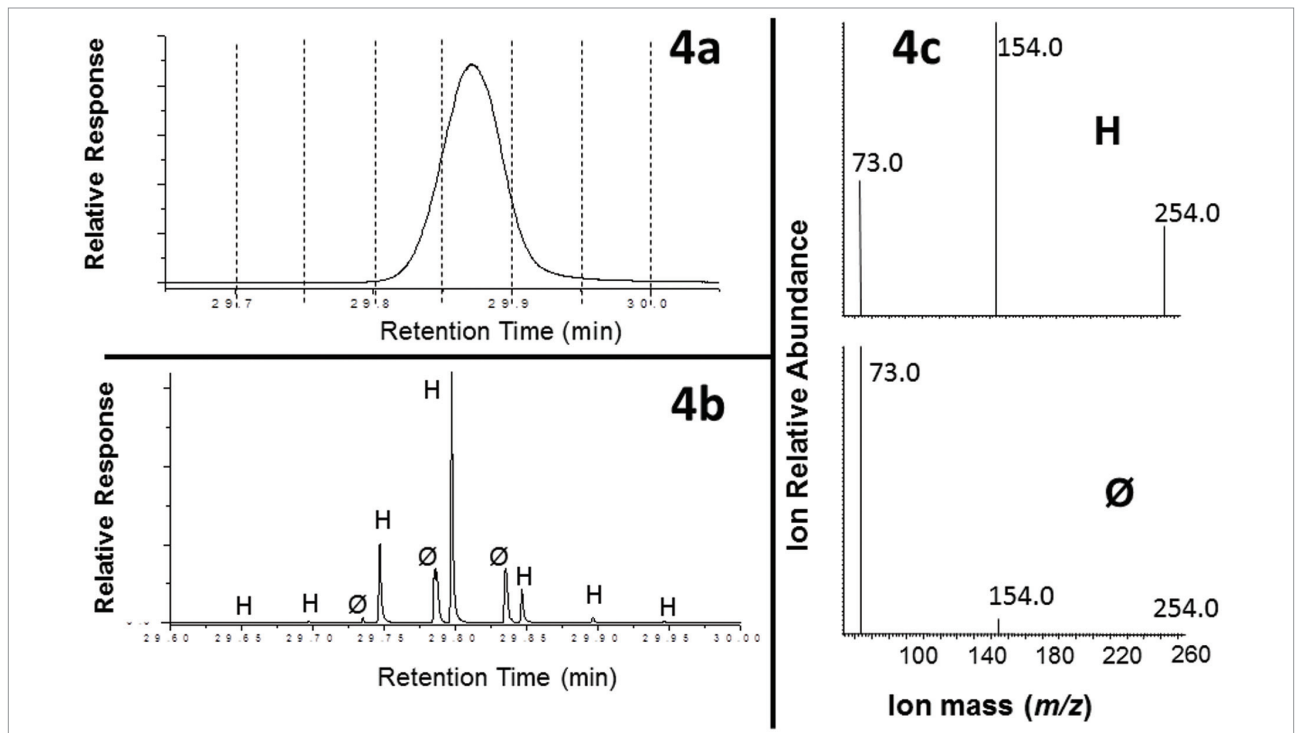


**Figure 4.** (a) The amino acid histidine peak comprises more than one component, which was not apparent from the 1D GC result. (b) The interfering peak ( $\emptyset$ ) is well separated from histidine (H) in the GC×GC analysis. Very small modulated peaks for histidine at the extremities of the peak are also readily seen as shown. (c) The mass spectrum of the interfering peak has ions in common with those of histidine, and so selected ion monitoring of histidine is not likely to be effective in providing unique analysis in 1D GC.

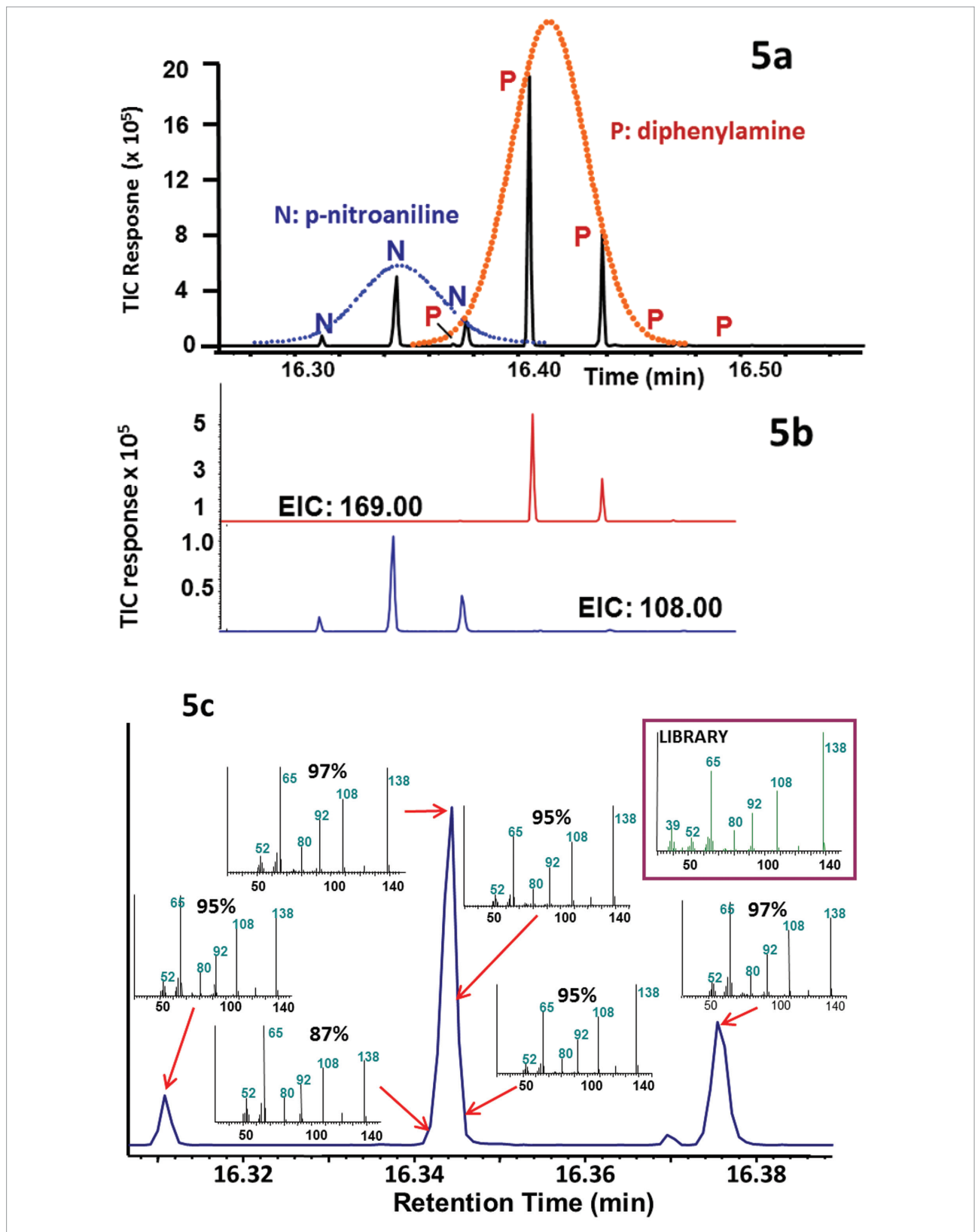


**Figure 5.** (a) p-nitroaniline and diphenylamine analysed by using GCxGC-qMS display acceptable peak shapes, which follow the Gaussian model for the pulsed peaks. (b) Extracted ion chromatograms of EIC  $m/z$  108 and  $m/z$  169 respectively are used to present the selected ion traces of the two compounds and confirm peak identity and attribution. (c) p-nitroaniline spectra acquired at points across the major modulated peak, and also at the peak maxima of the three modulated peaks. Peaks display shape indicative of the slow QMS sampling.

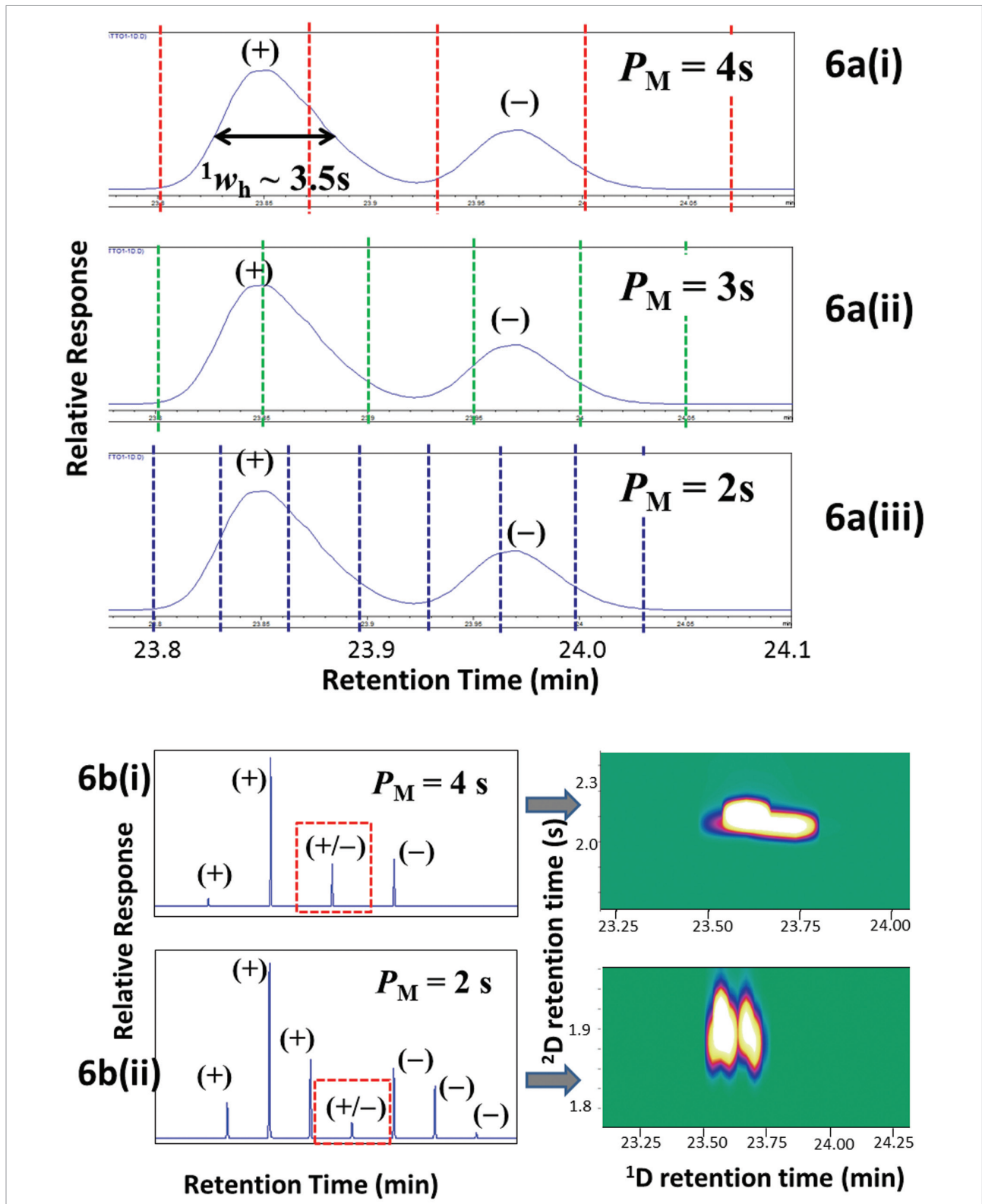


**Figure 6.** (a) The 1D analysis of (+)- and (-)-terpinen-4-ol ((+) and (-) respectively) shows that they are not completely resolved. The  $1w_h$  value is about 3.5 s. Indicative modulation sequences of  $P_M = 2\text{ s}$ , 3 s and 4 s events are shown superimposed on the 1D peaks. The  $M_R$  values are 2.8, 1.8 and 1.4 respectively. (b) The modulated peak distribution (bi) shows that there is a significant overlap of (+) and (-) for  $P_M = 4\text{ s}$ , but it is less significant for  $P_M = 2\text{ s}$ . The GC×GC 2D plot shows relatively good peak presentation for  $P_M = 2\text{ s}$  showing two 'nodes', but for  $P_M = 4\text{ s}$  rather than a clear presentation of two components, a single peak is apparently displayed.

### 3. Results and Discussion

#### 3.1. Modulation ratio and phase, number of observed peaks, and Gaussian peak shapes

A model for the effect of phase of modulation is shown in Figure 1<sup>[11]</sup>. A peak at the outlet of the <sup>1</sup>D column (a(i)) is delayed (this delayed time is referred to here as  $t_D$ ) by both the cryotrapping modulation residence time ( $P_M$ ), and the elution time on the <sup>2</sup>D column ( $t_R$ ), to give the total time for each modulated peak. The limiting cases of in-phase and 180° out-of-phase modulation are also illustrated (a(ii) and a(iii), respectively), giving two symmetric distributions with either one or two maximum peaks respectively. Some other options for peak modulation that give asymmetric peak distributions are shown here. In an experiment that progressively alters the commencement of the modulator for repeat injections, by 0.01 min, (this was achieved by starting the modulation process at for instance, 5.00, 5.01, 5.02 etc. min) it is possible to step the modulation pattern through various patterns, and identify approximate instances of in-phase (b(ii)), out-of-phase (b(v)), and various asymmetric cases. This is given in Figure 1b. This experiment can only be conducted if both the GC conditions and the modulation process is highly reproducible.

Figure 2 demonstrates different modulated patterns that may be obtained for a <sup>1</sup>D peak of  $w_h = 12$  s, as the modulation period is altered. The <sup>1</sup>D peak is illustrated here, for reference.

Each of these is obtained for a different  $P_M$  setting, as indicated in the caption. Also shown is a count of the total number of ‘modulated pulses’ that may be recorded for each  $P_M$  setting. This is termed the number of modulations ( $n_M$ ). It can be deduced from this that  $n_M$  will be difficult to accurately define if phase changes, since sometimes  $n_M$  is the same for different  $P_M$  settings, or may be different for the same  $P_M$  settings, if phase varies. Additionally, if less sample is injected, the modulations at the periphery will become indistinguishable from noise. Conversely, as more sample is injected, we may

start to observe more modulated peaks at the ‘wings’ of the <sup>1</sup>D peak. Thus  $n_M$  varies rather inconsistently for a compound and depends on the conditions of the analysis. Alternatively, also presented is the  $M_R$  value for each  $P_M$  setting. These are easily derived, since in this case each repeat injection presents an input peak with the same width, so  $M_R$  can be precisely determined, and progressively decreases as  $P_M$  increases; as  $P_M$  changes from 3s, 4s, 5 s, 6 s, to 7 s,  $M_R$  decreases from 6.8, 5.1, 4.1, 3.4 and 2.9. In terms of the major modulated peaks that are generated in this example, we see about 7, 5, 4, 3, and 2-3 peaks, respectively. For Figure 2a an almost in-phase modulation arises, and as shown by the lines, the modulated peaks after the maximum peak all are slightly smaller than the peaks before the maximum, as expected for a Gaussian <sup>1</sup>D peak input. The final case (Figure 2e) illustrates a distribution that is almost 180° out-of-phase, with two main peaks symmetrically located about the <sup>1</sup>D peak maximum, and two small peaks at the extremities. For a  $M_R$  of 2.9, an in-phase modulation will, however, give 3 major peaks. This number of peaks will closely represent the bulk of the area within the series of modulated peaks.

It is possible to draw exactly the same simulated Gaussian peak for each of these distributions, as must be the case. We can illustrate this by overlaying the initial Gaussian peak onto the modulated peaks. Each of the modulated examples is presented with the same time scale of 25.6 – 26.3. So by a cut-and-paste process, it should be possible to fit the input peak shape onto the modulated peaks (as in Figure 1a), with the only adjustment being to alter the intensity of the signal. What can be seen from the result here is that the position of the maximum of the overlaid peak shifts a little to the right for each increased  $P_M$  setting. This will be discussed later.

One question that arises, especially when dealing with detectors with limited acquisition speed, is the relationship between peak width and modulation ratio. For detectors with fast acquisition speed like FID or time-of-flight mass spectrometers with fast acquisition

speed, it will not be a problem if a proper acquisition rate is selected in the method. On the other hand, for lower acquisition speed detectors such as quadrupole mass spectrometers, if the number of data points collected per peak is limited, small differences in peak width may be important. The only way to cater for slow data acquisition is to have a compound elute into the detector more slowly, if a given number of data points are required per peak. If the  $M_R$  value of e.g. 3 is to be maintained, the only option is to have the  $^1D$  peak to be excessively broadened. This may be difficult to achieve experimentally. In the present example, the most prominent peak in each chromatogram presented peak widths at baseline of 200 ms. It means that the modulation ratio does not affect the  $^2D$  peak width with the type of modulator used here.

With fewer modulations across a peak, the response height will increase which has been well reported for GC×GC<sup>[11,17,18]</sup>. Figure 2 illustrates that as  $P_M$  is reduced (slower sampling), giving fewer modulations, overall response increases. Thus Figure 2a ( $P_M = 3$  s) has a maximum response of about 47 pA, but Figure 2d ( $P_M = 6$  s) has a major modulated peak response of about 100 pA. Interestingly, Figure 2e has even slower modulation ( $P_M = 7$  s), but the effect of phase of modulation now gives two reasonably tall peaks, so they have a slightly shorter response than for  $P_M = 6$  s. This simply is determined by how much of the initial  $^1D$  peak is sampled at any given event. The case of response increase of 1D GC vs. GC×GC can be seen for a typical sample analysis shown in Figure 3, where a dilute sample was injected into a GC instrument to give a result close to detection limit (e.g. the 1D result for component 12 = 3 x noise level, based on the definition where LoD is the concentration giving a signal = 3 x noise). The subsequent GC×GC analysis of a sample further diluted 2.5 fold gives a result that significantly exceeds the S/N level. From this we estimate an increase in S/N of 20 fold. This will be further discussed below.

### 3.2. Histidine, $M_R$ and a limited acquisition rate detector: quadrupole mass spectrometer

The key capabilities of GC×GC, such as in multidimensional gas chromatography are often reported as improved separation power<sup>[16]</sup>, increased sensitivity, and a unique structured retention that relates the position of peaks in 2D space to their molecular structure or chemical composition<sup>[19]</sup>.

Added to this might be general improved selectivity of detection, arising from the removal of underlying chemical interference, either from matrix, other target analytes, or even phase bleed. This should translate to better quality mass spectrometry, with consequent greater confidence of structure elucidation based on MS. In addition to the benefits of cryogenic focusing, this should add to improved detectability. Amino acid analysis provides an early example in GC×GC where analysis of a class of compounds of relevance to metabolomics can be readily applied to GC×GC<sup>[20]</sup>. As an example, consider the analysis of the trimethylsilyl derivative of the amino acid, histidine<sup>[21]</sup>. Firstly, analysis of a standard of 10 mg L<sup>-1</sup> histidine using splitless injection is shown in Figure 4.

The  $^1D$  peak is shown in Figure 4a to be modulated with  $M_R \sim 2$  (refer to the vertical dashed lines). With close to in-phase modulation (Figure 4b), the single central maximum, and smaller minor components with some asymmetry is noted. Whilst the  $^1D$  peak does not suggest the presence of an impurity, the impurity ( $\emptyset$ ) is clearly shown in the modulated trace (Figure 4b), in addition to the histidine peak (H). Mass spectra of both components H and  $\emptyset$  (Figure 4c) suggest that this might be difficult to identify in the absence of GC×GC due to the presence of similar ions. Library match summary data for all 7 of the modulated peaks, and the maximum ion abundance for each of the diagnostic ions  $m/z$  73, 154 and 254, for this example are presented in Table 1. Some points to note include that the relative ratios of the three ions are very similar for spectra recorded at the peak maxima for each modulated peak; it was noted

**Table 1.** Data for modulated peaks for Histidine, in GC×GC operation, using  $P_M = 0.05$  min (3 s). Refer to Figure 4 for the original chromatographic peak (Figure 4a) and the modulated peaks (Figure 4b).

Modulated peak number	Peak 1	Peak 2	Peak 3	Peak 4	Peak 5	Peak 6	Peak 7	
Peak $t_R$ (min)	29.647	29.697	29.747	29.797	29.847	29.897	29.947	
Ion abundance	$m/z$ 73	$1.26 \times 10^4$	$3.14 \times 10^4$	$1.31 \times 10^6$	$3.57 \times 10^6$	$6.20 \times 10^5$	$7.05 \times 10^4$	$3.63 \times 10^4$
	$m/z$ 154	$1.89 \times 10^4$	$4.44 \times 10^4$	$2.85 \times 10^6$	$8.39 \times 10^6$	$1.19 \times 10^6$	$1.19 \times 10^5$	$5.72 \times 10^4$
	$m/z$ 254	$0.60 \times 10^4$	$1.28 \times 10^4$	$8.67 \times 10^5$	$3.53 \times 10^6$	$3.43 \times 10^5$	$3.42 \times 10^4$	$1.65 \times 10^4$
Rel ratio vs $m/z$ 154 ion total*	0.15%	0.35%	22.49%	66.22%	9.39%	0.94%	0.45%	

\*The relative ratios of each of the modulated pulses vs the ions  $m/z$  73 and  $m/z$  254 are similar.

that spectrum matching with histidine was acceptable for each. Also, not only are the major 3 peaks presented, but fully all 7 peaks have been correctly identified for the modulated histidine compound. This is perhaps a very surprising result – that 7 peaks can be seen for a component with a  $M_R$  value of about 2, for a  $10 \text{ mg L}^{-1}$  injected solution.

Some further quantitative interpretation can be offered. Taking the relative proportions of ion abundance for the  $m/z$  154 ion, which equals  $1.270 \times 10^7$ , this may be equated to a total of  $10 \text{ mg L}^{-1}$ . The same interpretation can be made for each of the other ions. This should then mean that about 66.2% of the total amount of compound resides in the major modulated peak, corresponding to  $6.6 \text{ mg L}^{-1}$ . It follows that the smallest peak has a relative concentration of  $0.015 \text{ mg L}^{-1}$  or  $15 \mu\text{g L}^{-1}$ . A similar interpretation can be followed for the other key ions (Table 1). Hence we can detect by qMS an amount of  $15 \mu\text{g L}^{-1}$  of amino acid corresponding to this peak. Note that SIM analysis is performed in this case. This is a very good result, and illustrates that qMS should offer sufficient sensitivity and by extension linearity for use with GC×GC. Detection linearity is indicated by the peak still maintaining a reasonable Gaussian shape, but is best measured by injection of a sample over a wide mass range.

### 3.3. Quadrupole MS, qualitative analysis and spectrum quality

Quadrupole MS was demonstrated to be useful for providing GC×GC data, and even with an instrument capable of up to  $12,000 \text{ amu/s}$  sampling rate, as used above, is capable of quantitative data and qualitative data in certain circumstances. Whilst it is beyond the present study to provide an extensive review of MS with GC×GC, a few pertinent prior studies will be mentioned. Frysinger and Gaines<sup>[22]</sup> used an older qMS with rather slow scanning (a few scans/s) with very long elution times to demonstrate that this technology was capable of application to GC×GC. Marriott and co-workers used reduced mass range scanning for applications to drugs analysis and essential oils<sup>[23,24]</sup>, where the reduced mass range allowed faster cycle time. They also used this for enantioselective analysis, in combination with vacuum conditions in the second column to speed up diffusion processes. Mondello's group<sup>[25]</sup>, and recently Weinert and coworkers<sup>[26]</sup> had access to faster scanning qMS, of up to  $20,000 \text{ amu/s}$ , to permit wider scan range and/or faster cycle times with GC×GC. This remains the fastest qMS option available.

It was shown above that for histidine, relatively good ion ratios were obtained at the peak maxima for each of the modulated peaks. For a mixture of *p*-nitroaniline and diphenylamine in GC×GC-qMS

(Figure 5) which partially overlap (Figure 5a), extracted ion data of  $m/z$  108 and 169 respectively illustrate the individual modulated peaks of the two compounds (Figure 5b). Expanded data for p-nitroaniline indicate that sampling of the data is relatively slow as shown by the lack of smoothness of the peaks (Figure 5c). Only about 6 data points are acquired across each peak. The skewing of peaks due to the qMS scanning can be gleaned from data points collected across the maximum modulated peak; MS library match quality data are 87%, 97%, 95% and 95% respectively. However at the peak maxima, data are 95%, 97% and 97% respectively, suggesting that good MS data quality is possible for qualitative analysis. On the other hand, for the use of quadrupole MS for quantitative analysis, it is important to observe that, for triplicate analysis of the same sample, with a reproducible modulation ratio, with reproducible number of registered data points per peak, the position of the data point collected in a low scan quadrupole may not be reproducible. In addition, skewing of mass spectra may be significant across each peak. For a fast scan quadrupole, acceptable results were presented for untargeted analysis of drug metabolites in urine samples, under specific conditions, considering a relatively high mass spectra skewing along the modulated peak, as presented by the authors<sup>[26]</sup>.

Franchina and coworkers<sup>[27]</sup> recently used GC×GC with a loop type modulator and a triple quadrupole instrument to semi-quantify aromatic sulfur containing compounds in heavy gas-oil, presenting consistent results with a low flow of mobile phase ( $0.3 \text{ mL min}^{-1}$ ), and acquisition rate of 25 Hz. In samples with such complexity, where the main focus is to quantify chemical classes of hundreds of isomers, modulation ratio may be useful to evaluate the systematic peak shape modulation profile of each chemical class. This information can be useful for mathematical data filtering to remove signal coming from column contamination, since repetitive modulations expected for a specific class can be filtered, as used by Weinert et al.<sup>[26]</sup>.

### 3.4. Summed modulated peaks: A chiral separation problem

If compounds cannot be resolved adequately on the <sup>1</sup>D column, they might still be well quantified if they are well resolved on the <sup>2</sup>D column. A problem arises if <sup>2</sup>D separation is not possible. In this case, if modulation collects the two compounds into the one event, then an unresolved single composite peak is obtained on <sup>2</sup>D. This can be minimized if a high  $M_R$  setting is used, in order to reduce the possibility of sampling the overlap region, but this critically depends on the severity of overlap. One solution will be to ensure peaks are fully resolved on the <sup>1</sup>D column, but this cannot always be guaranteed.

Amador-Munoz and Marriott<sup>[28]</sup> studied polyaromatic hydrocarbons (PAH) and their per-deuterated analogue internal standards in atmospheric air extracts from Mexico city. The PAH and d-PAH were almost fully resolved, but some small measure of overlap was observed. Based on the concepts outlined by Khummeung et al.<sup>[6]</sup>, it was further decided<sup>[9]</sup> to investigate sampling only a subset of the modulated peaks. Thus both 2 and 3 modulated peaks were tested, and it was determined that summing 3 peaks for each analyte proved to be adequate for quantification.

More recently, Wong et al.<sup>[29]</sup> applied this same approach to insufficiently resolved enantiomers on a first enantioselective column in *e*GC×GC (*e* refers to the first column being enantioselective). The <sup>2</sup>D achiral column cannot resolve the enantiomers. In some cases, it is simply not possible to resolve all enantiomers by using a single enantioselective GC phase, and so a strategy to provide quantitative assessment is necessary. Mass spectra deconvolution capability of a powerful mass spectrometer, or high resolution mass spectrometry will be useless in this case. In the stated example, a multidimensional gas chromatography method did provide adequate resolution of the enantiomers, but a comparative *e*GC×GC approach was also sought.

Figure 6 presents a summary of the data for the *e*GC×GC of terpinen-4-ol<sup>[29]</sup>. The <sup>1</sup>D separation, with

various series of modulations using different  $P_M$  settings, are shown as overlay of the  $^1D$  peaks (Figure 6a(i-iii)) = 4, 3 and 2 s respectively). Figure 6b(i) and (ii) display the result for GC×GC using  $P_M$  of 4 s and 2 s respectively, first for the linear data display, and also for the 2D plot presentations of the resulting data. Clearly,  $P_M = 4$  s presents a very indistinct 2D plot. How the overlap peak (shown as (+/-)) is handled presents some options, all of which suffer from various shortcomings. The overlap peak can be equally apportioned to both enantiomers; the overlap peak can be fully attributed to one of the isomers (e.g. the more intense enantiomer); the overlap peak can be simply ignored, and quantification can be based on the summed response of the largest 2 or 3 pure enantiomer peaks. Clearly, phase of modulation will play a role in these cases. In the example here, using the shortest  $P_M$  gives the smallest overlap peak, and will in all cases give the best possible measure of chiral ratio of the terpinen-4-ol compound. The 2D plot in Figure 6b(ii) shows the best differentiation of the two enantiomer peaks.

### 3.5. Predicting an accurate first dimension retention time

Although not strictly associated with the concept of the modulation ratio, predicting a first dimension retention with greater accuracy than is often reported for the  $^1D$  time in GC×GC is important, since it recovers a degree of precision and accuracy for the  $^1D$  retention that is lost if a  $^1D$  time ( $^1t_R$ ) is given with a precision derived from the modulation period used in the experiment. All chromatographic analyses have retention as a basic parameter that strictly describes the interaction between the solute and the phase. It is the very parameter that relates to the chemistry of the compound, is reported in almost every paper published in chromatography, and one expects that just because a new technique is developed, the value of retention should not simply be reduced in importance.

If GC×GC compromises the peak capacity on the first column due to the modulation process, by leading to uncertainty in the quality of the  $^1D$  separation, then

by developing a metric to increase accuracy of the  $^1D$  retention, this overcomes some degree of this uncertainty. For instance, peak capacity of a GC×GC experiment is given by  $n_T = ^1n_c \times ^2n_c$ , and is further modified to take into account the modulation process by a factor that reduces the total value<sup>[30]</sup>. By more accurately quoting  $^1t_R$  it should be possible to re-assess the total capacity consideration, by simply reporting the total peak space in a 2D plot in terms of retention precisions. This concept requires further exploration.

The method to calculate a more accurate  $^1t_R$  is based on the  $^1D$  Gaussian peak as shown in Figure 1, fitting the modulated peak distribution to the Gaussian, and deriving the peak maximum of this Gaussian. The peak maximum possesses the classical information of the Gaussian, which includes the peak standard deviation. This works best for a Gaussian peak, but with some additional consideration can apply to an asymmetric peak. This was considered by Ong<sup>[11]</sup>, proposed by Shellie et al.<sup>[12]</sup> and further modified by Adcock et al.<sup>[13]</sup>.

### 3.6. GC×GC improves detection limits in GC analysis

The tenets of and rationalisation for developing GC×GC methods include (i) a greater use of separation space arises from the 2D presentation format, which is due to significant peak capacity increase, (ii) limit of detection of compounds (LoD) decreases due to the cryogenic modulation approach which is the most common implementation method for GC×GC, and (iii) the 2D space locates related compounds in unique patterns of retention – referred to as structured retentions – due to the similar chemical nature of the compounds<sup>[19]</sup>. The first two of these are general desirable performance criteria for any new method development. The goal of better separation and lower LoD is fundamental to chromatographic advances. Analytical response for LoD calculations can be viewed in terms of peak area or peak height. A detector usually has an associated detectability, normally given as mass per time, e.g. ng of injected material per s of time that the peak elutes into the detector

(e.g. approximated by the peak width at baseline). For a given detector, capillary GC columns therefore provide lower detection limits than for packed columns, due to the narrower peaks in the former. Similarly, for GC×GC, peaks are modulated into a distribution of sharp pulses, and since they are much narrower, they will allow detection to a lower mass. Since the GC×GC process preserves peak transfer from  $^1\text{D}$  to  $^2\text{D}$ , the same mass of compound should yield the same peak area in 1D GC or GC×GC. However the peak response height should be much greater. Although the total area does not increase when using GC×GC, the important parameter is whether the individual modulated peaks can be 'seen' above the S/N limit of 3, for cases where the 1D GC peak is not detected. Anecdotal evidence from many GC×GC users is that it is possible to record peaks in GC×GC when no peak is evident for an equivalent 1D GC analysis.

How much improvement is possible? Consider a GC peak of 5 s width. If the cryogenic modulator focusses the peak to a sharp band, and releases it to  $^2\text{D}$  in a band of e.g. 10 ms, this corresponds to a 500-fold increase in concentration per time. After traversing the  $^2\text{D}$  column, the peak width may be about 200 ms wide; this still corresponds to about 25-fold magnitude increase. Since a faster eluting peak requires faster data acquisition frequency detection, this increases detector noise level. If the detector frequency is increased 10-fold (e.g. from 5 Hz to 50 Hz), this increases noise by about 3-fold. Hence net S/N will be about  $25/3 = 8$  times improvement in detection limits.

But we have to consider both modulation ratio and phase of modulation here. Thus in the simplest case, if  $M_{\text{R}} \sim 1$ , with in-phase modulation, most peak area is captured into a single peak. So an 8-fold improvement should be possible (but care is needed with respect to overloading of the  $^2\text{D}$  column, since mass flux per time unit will increase). If  $180^\circ$  out-of-phase modulation occurs, the peak is split into two equal portions, so a 4-fold increase might be expected. However if  $M_{\text{R}}$  is very large, e.g. 10, then many modulations arise, and

there a diminishingly smaller improvement in detection since not much of the  $^1\text{D}$  peak is concentrated into the major modulated peak. Since most practitioners use  $M_{\text{R}}$  values around 2-4, then LoD improvements about 5 fold might be anticipated.

Liu et al.<sup>[31]</sup> reported analysis of pesticides by using the GC×GC-FPD (P-mode). This detector proved to be an excellent method for GC×GC peaks, since it is capable of very fast acquisition ( $> 200$  Hz), and the transducer generates peaks in all respects very similar to that of the FID<sup>[32]</sup>. It is also very sensitive, and is selective to P-containing compounds. LoD in GC×GC was from  $1.5 \mu\text{g L}^{-1}$  to  $5.6 \mu\text{g L}^{-1}$ , whereas for 1D GC analysis levels from  $8.8 \mu\text{g L}^{-1}$  and  $13.6 \mu\text{g L}^{-1}$  were found. Engel et al.<sup>[33]</sup> contrasted a range of selective detectors (FPD(S); FPD(P); ECD; NPD and ToFMS) for the analysis of a large number of pesticides, and reported that LoD were not significantly reduced for GC×GC.

Krupcik et al.<sup>[34]</sup> applied the standard IUPAC criteria for LoD and LoQ to GC×GC data, with FID. They stated that GC×GC improves sensitivity by about 3-fold, considering the S/N ratio and the peak high of the most prominent peak. Rephrasing their conclusion, but with the modulation ratio concept, the best LoD can be achieved with the lower  $M_{\text{R}}$  applicable without compromise the selectivity. In other words, without sacrificing the  $^1\text{D}$  separation and  $^2\text{D}$  column overloading. They also noted that since the distribution pattern of modulated peaks for GC×GC is random and cannot be predicted (modulation phase), and the peak height for the most prominent peak in an in-phase modulation is 30% higher than the closest peaks for their examples, LoQ and LoD may vary within 30% for 3 s modulation time. On the other hand, the authors did not present the precision of those results based on repetitive analysis. If the  $M_{\text{R}}$  was 1, this comparison could not be performed, and this number could not be predicted. If the  $M_{\text{R}}$  was higher than the observed, or the ratio between the monodimensional peak height and peak width was different, this value may also be different. An interesting study will include the

% variation observed with selected  $M_R$  values, and also studying peaks with different peak height/peak width ratios.

Franchina and coworkers<sup>[27]</sup> used the highest modulated peak as reference for LoD, not taking into account the modulation ratio. On the other hand, they developed the separation method in order to have a minimum peak width to allow a significant number of data points per peak. They observed an intra-day precision for the lowest calibration point to be between 7 and 17%. Those observations may vary from one equipment to another, since the reproducibility of modulation phase is dependent on the type of modulator, the stability of the stationary phases and the chemistry of the analyte, regarding interaction with the stationary phase. Using different  $M_R$  will also play an important role in those results since the % of the area of the total peak in the higher modulated peak will be different if a lower or higher  $M_R$  is used.

The best approach to establish LoD and LoQ in GC×GC is still in discussion in the literature, and little has been done in respect to the influence of  $M_R$  on LoD values and precision.

One important discussion that often arises in 1D GC is the use of the S/N approach for selected ion monitoring with mass spectrometry detectors, since the noise for a selected mass can be zero in several cases. In our opinion the most recommended approach to be applied in any 1D GC or multidimensional GC separation is the use of the statistical data of a calibration curve, since it demonstrates if the LoQ is valid for the applied conditions<sup>[34]</sup>.

## 4. Conclusion

GC×GC occupies a unique position in both the technology and lexicon of gas chromatography. This work has shown that many properties regarding the implementation of GC×GC can be based on interpretation of the modulation ratio,  $M_R$ . Thus the number of ‘major’ modulated peaks that can be expected is similar to the  $M_R$  value; detection limits need to be interpreted paying cognisance to  $M_R$ ; it is possible to determine quantitative data by summing a certain number of modulated peaks and the  $M_R$  determines how many peaks need to be summed in order to obtain a desired % of peak area; by considering the distribution of peaks it is possible to predict the retention time on the first dimension column;  $M_R$  also can aid optimisation of the GC×GC experiment to determine the maximum retention allowed on the 2D column. Along with terms such as modulation period, phase of modulation, contour plot and peak apex plot, modulation ratio now assists analysts to define their GC×GC experiment. This article intends to bring a number of different studies related to  $M_R$  together to discuss the role that  $M_R$  plays in setting a context for the experiment, independently of the type of modulator or detector used. It also suggests that the influence of  $M_R$  on the evaluation of LoD precisions has not been evaluated in the literature, to the best of our knowledge.

## Acknowledgements

PJM acknowledges funding from the ARC Discovery and Linkage program grants DP130100217 and LP130100048. PJM acknowledges ARC funding for a Discovery Outstanding Researcher Award. PJM also acknowledges CNPq for funding through program 314511/2014-8.

## References

- [1] Liu Z, Phillips JB. Comprehensive two-dimensional gas chromatography using an on-column thermal modulator interface. *J Chromatogr Sci.* 1991;29(6):227-31.
- [2] Chin S-T, Marriott PJ. Multidimensional gas chromatography beyond simple volatiles separation. *Chem Commun.* 2014;50:8819-33.
- [3] Meinert C, Meierhenrich UJ. A new dimension in separation science: Comprehensive two-dimensional gas chromatography. *Angew Chem Int Ed.* 2012;51:10460-70.
- [4] Schoenmakers P, Marriott P, Beens J. Nomenclature and conventions in comprehensive multidimensional chromatography. *LC-GC Europe.* 2003;June:1-4.
- [5] Marriott PJ, Wu Z, Schoenmakers P. Nomenclature and conventions in comprehensive multidimensional chromatography – an update. *LC-GC Europe.* 2012;25:266-75.
- [6] Khummueng W, Harynuk J, Marriott PJ. Modulation ratio in comprehensive two-dimensional gas chromatography. *Anal Chem.* 2006;78(13):4578-87.
- [7] Khummueng W, Marriott PJ. The nomenclature of comprehensive two-dimensional gas chromatography: Defining the modulation ratio ( $M_r$ ). *LC-GC Europe.* 2009;22(1):38-43.
- [8] Harynuk JJ, Kwong AH, Marriott PJ. Modulation-induced error in comprehensive two-dimensional gas chromatographic separations. *J Chromatogr A.* 2008;1200:17-27.
- [9] Amador-Munoz O, Marriott PJ. Quantification in comprehensive two-dimensional gas chromatography and a model of quantification based on selected summed modulated peaks. *J Chromatogr A.* 2008;1184(1-2):323-40.
- [10] Harynuk J, Gorecki T, Zeeuw Jd. Overloading of the second-dimension column in comprehensive two-dimensional gas chromatography. *J Chromatogr A.* 2005;1071(1-2):21-7.
- [11] Ong R, Marriott P. A review of basic concepts in comprehensive two-dimensional gas chromatography. *J Chromatogr Sci.* 2002;40:276-91.
- [12] Shellie RA, Xie L-L, Marriott PJ. Retention time reproducibility in comprehensive two-dimensional gas chromatography using cryogenic modulation. An intralaboratory study. *J Chromatogr A.* 2002;968(1-2):161-70.
- [13] Adcock JL, Adams M, Mitrevski BS, Marriott PJ. Peak modeling approach to accurate assignment of first-dimension retention times in comprehensive two-dimensional chromatography. *Anal Chem.* 2009;81(16):6797-804.
- [14] Marriott PJ, Kinghorn RM. Longitudinally modulated cryogenic system. A generally applicable approach to solute trapping and mobilization in gas chromatography. *Anal Chem.* 1997;69(13):2582-8.
- [15] Kinghorn RM, Marriott PJ. Comprehensive two-dimensional gas chromatography using a modulating cryogenic trap. *J High Resol Chromatogr.* 1998;21(11):620-2.
- [16] Marriott PJ, Chin S-T, Maikhunthod B, Schmarr H-G, Bieri S. Multidimensional gas chromatography. *TrAC Trends Anal Chem.* 2012;34:1-21.
- [17] Lee AL, Bartle KD, Lewis AC. A model of peak amplitude enhancement in orthogonal two-dimensional gas chromatography. *Anal Chem.* 2001;73(6):1330-5.

- [18] Mitrevski BS, Wilairat P, Marriott PJ. Comprehensive two-dimensional gas chromatography improves separation and identification of anabolic agents in doping control. *J Chromatogr A*. 2010;1217(1):127-35.
- [19] Marriott PJ, Massil T, Hugel H. Molecular structure retention relationships in comprehensive two-dimensional gas chromatography. *J Sep Sci*. 2004;27:1273-84.
- [20] Mayadunne R, Nguyen T-T, Marriott PJ. Amino acid analysis by using comprehensive two-dimensional gas chromatography. *Anal Bioanal Chem*. 2005;382(3):836-47.
- [21] Yang SO, Choi HK, Marriott PJ. unpublished observations 2009.
- [22] Frysinger GS, Gaines RB. Comprehensive two-dimensional gas chromatography with mass spectrometric detection (GC x GC/MS) applied to the analysis of petroleum. *J High Resol Chromatogr*. 1999;22(5):251-5.
- [23] Song SM, Marriott P, Wynne P. Comprehensive two-dimensional gas chromatography-quadrupole mass spectrometric analysis of drugs. *J Chromatogr A*. 2004;1058(1-2):223-32.
- [24] Shellie RA, Marriott PJ, Huie CW. Comprehensive two-dimensional gas chromatography (GC × GC) and GC × GC-quadrupole MS analysis of Asian and American ginseng. *J Sep Sci*. 2003;26(12-13):1185-92.
- [25] Purcaro G, Tranchida PQ, Ragonese C, Conte L, Dugo P, Dugo G, et al. Evaluation of a rapid-scanning quadrupole mass spectrometer in an apolar x ionic-liquid comprehensive two-dimensional gas chromatography system. *Anal Chem*. 2010;82(20):8583-90.
- [26] Weinert CH, Egert B, Kulling SE. On the applicability of comprehensive two-dimensional gas chromatography combined with a fast-scanning quadrupole mass spectrometer for untargeted large-scale metabolomics. *J Chromatogr A*. 2015;1405:156-67.
- [27] Franchina FA, Machado ME, Tranchida PQ, Zini CA, Caramão EB, Mondello L. Determination of aromatic sulphur compounds in heavy gas oil by using (low-)flow modulated comprehensive two-dimensional gas chromatography–triple quadrupole mass spectrometry. *J Chromatogr A*. 2015;1387:86-94.
- [28] Amador-Muñoz O, Villalobos-Pietrini R, Aragón-Piña A, Tran TC, Morrison P, Marriott PJ. Quantification of polycyclic aromatic hydrocarbons based on comprehensive two-dimensional gas chromatography-isotope dilution mass spectrometry. *J Chromatogr A*. 2008;1201(2):161-8.
- [29] Wong YF, West RN, Chin S-T, Marriott PJ. Evaluation of fast enantioselective multidimensional gas chromatography methods for monoterpene compounds: Authenticity control of Australian tea tree oil. *J Chromatogr A*. 2015;1406:307-15.
- [30] Klee MS, Cochran J, Merrick M, Blumberg LM. Evaluation of conditions of comprehensive two-dimensional gas chromatography that yield a near-theoretical maximum in peak capacity gain. *J Chromatogr A*. 2015;1383:151-9.
- [31] Liu X, Mitrevski B, Li J, Li D, Marriott PJ. Comprehensive two-dimensional gas chromatography with flame photometric detection applied on organophosphorus pesticides in food matrices. *Microchem J*. 2013;111:25-31.
- [32] Chin ST, Wu ZY, Morrison PD, Marriott PJ. Observations on comprehensive two dimensional gas chromatography coupled with flame photometric detection for sulfur- and phosphorus-containing compounds. *Anal Meth*. 2010;2(3):243-53.
- [33] Engel E, Ratel J, Blinet P, Chin S-T, Rose G, Marriott PJ. Benchmarking of candidate detectors for multiresidue analysis of pesticides by comprehensive two-dimensional gas chromatography. *J Chromatogr A*. 2013;1311:140-8.
- [34] Krupčík J, Májek P, Gorovenko R, Blasko J, Kubinec R, Sandra P. Considerations on the determination of the limit of detection and the limit of quantification in one-dimensional and comprehensive two-dimensional gas chromatography. *J Chromatogr A*. 2015;1396:117-30.